

Science, Vol.316, p.1169, 2007

An On-Demand Coherent Single Electron Source

G. Fève,¹ A. Mahé,¹ J.-M. Berroir,¹ T. Kontos,¹ B. Plaçais,¹ D.C. Glattli,^{1,2,*}

A. Cavanna,³ B. Etienne,³ Y. Jin³

¹Laboratoire Pierre Aigrain, Département de Physique de l'École Normale Supérieure

24 rue Lhomond, 75231 Paris Cedex 05, France

²Service de Physique de l'Etat Condensé, CEA Saclay

F-91191 Gif-sur-Yvette, France

³Laboratoire de Photonique et Nanostructures, UPR20 CNRS

Route de Nozay, 91460 Marcoussis Cedex, France

* To whom correspondence should be addressed; E-mail: glattli@lpa.ens.fr.

We report on the electron analog of the single photon gun. On demand single electron injection in a quantum conductor was obtained using a quantum dot connected to the conductor via a tunnel barrier. Electron emission is triggered by application of a potential step which compensates the dot charging energy. Depending on the barrier transparency the quantum emission time ranges from 0.1 to 10 nanoseconds. The single electron source should prove useful for the implementation of quantum bits in ballistic conductors. Additionally periodic sequences of single electron emission and absorption generate a quantized AC-current.

In quantum optics, a single photon source is an essential building block for the manipulation of the smallest amount of information coded by a quantum state: a qubit [1, 2]. Combined with beam-splitters, polarizers and projective measurements several photonic qubits can be manipulated to process quantum information [3]. The most celebrated case is the secured transmission of the information using quantum cryptography. Similarly, one expects that electrons propa-

gating ballistically in ultra-pure low dimensional conductors can realize quantum logic tasks in perfect analogy with photons propagating in optical media [4, 5, 6]. The analogy has a long history [7] and has provided illuminating comparisons between the intensity of light and that of electrical current, between photon noise and electrical shot noise [8, 9] and more recently between photon and electron quantum entanglement [10, 11, 12]. Interestingly, electrons being Fermions, entanglement offers new routes not possible with photons [12]. Practically, electronic analogs of beam-splitters, Fabry-Pérot and Mach-Zehnder interferometers [13, 14] have been realized in ballistic conductors providing the necessary quantum gate for an 'all linear' electron optics quantum computation. Yet missing were the single electron source and the single electron detector [15] suitable for coherent emission and projective measurements. The former initializes quantum states, while the latter reads the final states after electrons have passed through the quantum gates.

Unlike the case of photons, realization of single electron sources is expected to be simpler because of Fermi statistics and Coulomb interaction. For example, considering a voltage biased single mode conductor, a contact at energy eV above the energy of the other contact is known to inject single electrons into the conductor at a regular rate eV/h , thereby leading to quantization of the dc current in Quantum Point Contacts [16, 17]. A second example is the electron pump where a dc current is produced by sequential time-controlled transfer of single electrons between metallic islands in series [18, 19] or manipulation of tunnel barriers of quantum dots [20, 21]. The cost in Coulomb charging energy to add or remove an electron ensures a well defined electron number in each island or dot. These two sources are however not useful for quantum information. In the first case, there is no time control of the electron injection. As only statistical measurements are possible, the biased contact is suitable for demonstrating coherent phenomena such as interferences or electron entanglement [10, 11] but not for manipulating quantum information. In the second example, time controlled injection can be realized, but the energy of emitted electrons is expected to spread, at random, in an energy range much larger than the tunneling rate (typically a fraction of the charging energy, depending on the pumping conditions). The statistical distribution in energy will smear coherent effects required for ma-

nipulating the quantum information. Finally, a third approach has been theoretically proposed in Refs. [22, 23, 24] considering voltages pulses $V(t)$ applied to an ohmic contact. When the Faraday flux $e \int V(t') dt' / h$ is an integer, an integer number of electrons is injected. Here noiseless injection requires to have a special Lorentzian shape of the pulse and exact integer value otherwise logarithmic divergence of the charge fluctuations occurs. No experiment is available yet to test these ideas.

We report on the realization of a time controlled single electron source suitable for coherent manipulation of ballistic electronic qubits which emits the electrons into a well defined quantum state. The injection scheme is different from those considered above. The source is made of a quantum dot, realized in a 2D electron gas in GaAs semiconductors, and tunnel-coupled to the conductor through a quantum point contact (QPC). By applying a sudden voltage step on a capacitively coupled gate, the charging energy is compensated and the electron occupying the highest energy level of the dot is emitted. The final state of the electron is a coherent wavepacket propagating away in the conductor. Its energy width is given by the inverse tunneling time, as required for on-demand single particle source, and independent on temperature. Its mean energy can be adjusted above the Fermi energy by tuning the voltage step amplitude. The circuit (Fig.1A), is realized in a 2D electron gas (2DEG) in a GaAsAl/GaAs heterojunction of nominal density $n_s = 1.7 \times 10^{15} \text{ m}^{-2}$ and mobility $\mu = 260 \text{ V}^{-1} \text{ m}^2 \text{ s}^{-1}$. The dot is electrostatically coupled to a metallic top gate, 100nm above the 2DEG, whose ac voltage, V_{exc} , controls the dot potential at the subnanosecond timescale. For all measurements, the electronic temperature is about 200 mK and a magnetic field $B \approx 1.3 \text{ T}$ is applied to the sample so as to work in the quantum Hall regime with no spin degeneracy. The QPC dc gate voltage V_G is tuned to control the transmission D of a single edge state as well as the dc dot potential. As reported [25], this circuit constitutes the paradigm of a quantum coherent RC circuit where coherence is seen to strongly affect the charge relaxation dynamics. From this study, the charging energy $\Delta + e^2/C \approx \Delta \approx 2.5 \text{ K}$ was extracted [26]. Here the large top gate capacitance makes the Coulomb energy e^2/C unusually small and the total charging energy identifies to the energy level spacing Δ .

In Ref.[25], the linear response of the current to the ac top gate voltage was investigated and the ac charge amplitude was much lower than the elementary charge e . Here, in order to achieve single charge injection we have to apply a high amplitude excitation ($V_{exc} \sim \Delta/e$) and go beyond the linear regime. When an electron is suddenly brought above the Fermi energy of the lead, it is expected to escape the dot at a typical tunnel rate $\tau^{-1} = D\Delta/h$, where Δ/h is the attempt frequency and D the transmission probability. This gives nanosecond timescales for which single charge detection is still out of reach experimentally. To increase the signal to noise ratio, a statistical average over many individual events is used by generating repetitive sequences of single electron emission followed by single electron absorption (or hole emission) as sketched in Fig.1A. This is realized by applying a periodic square wave voltage amplitude $\approx \Delta/e$ to the top gate. Fig.1B shows typical temporal traces of the current averaged over few seconds for a repetition period of $\mathcal{T} = 32 \text{ ns}$. The single electron events remarkably reconstruct the exponential current decay of an RC circuit. When decreasing transmission D from ≈ 0.03 to ≈ 0.002 , the relaxation time τ , extracted from the exponential decay, increases from 0.9 ns to 10 ns. For the two highest transmissions in Fig.1B, $\tau \ll \mathcal{T}/2$, the current decays to zero and the mean transferred charge per half period is constant. For the smallest transmission, $\tau \sim \mathcal{T}/2$, the mean emitted charge decreases as electrons have reduced probability to escape the dot. These time-domain measurements are limited by the 1 GHz bandwidth of the acquisition card and give access to the few nanoseconds injection times corresponding to small transmissions $D \lesssim 0.03$.

In order to get a better understanding of the above results, we extend the harmonic linear response theory of a quantum RC circuit [27, 28, 29] to calculate the non-linear response to a high amplitude square excitation voltage ($eV_{exc} \gg hf$). Calculation shows that the circuit still behaves as an RC circuit with a current given by:

$$I(t) = \frac{q}{\tau} e^{-t/\tau} \quad \text{for } 0 \leq t \leq \mathcal{T}/2 \quad (1)$$

$$q = e \int d\epsilon N(\epsilon) [f(\epsilon - 2eV_{exc}) - f(\epsilon)] \quad (2)$$

$$\tau = \frac{h \int d\epsilon N(\epsilon)^2 [f(\epsilon - 2eV_{exc}) - f(\epsilon)]}{2 \int d\epsilon N(\epsilon) [f(\epsilon - 2eV_{exc}) - f(\epsilon)]} \quad (3)$$

where $N(\epsilon)$ is the dot density of states and $f(\epsilon)$ denotes the Fermi-Dirac distribution. The non-

linear capacitance and charge relaxation resistance can be defined respectively by $\widetilde{C}_q \equiv q/2V_{exc}$ and $\widetilde{R}_q \equiv \tau/\widetilde{C}_q$. For unit transmission $D = 1$, electrons are fully delocalized, $N(\epsilon)$ is uniform and the charge q evolves linearly with V_{exc} as expected. At the opposite, for low transmission, $N(\epsilon)$ is sharply peaked on well resolved energy levels, and q exhibits a staircase dependence on V_{exc} with steep steps whenever one electronic level is brought above the Fermi energy. Thus our calculations establish the sketch of single electron injection depicted in Fig.1. For a dot energy spectrum with constant level spacing Δ , a remarkable situation occurs when $2eV_{exc} = \Delta$, as $q = e$ and $\widetilde{C}_q = e^2/\Delta$ irrespective of the transmission D and of the dc dot potential. As a matter of fact, Eq.2 shows that, in these conditions, q is given by integrating $N(\epsilon)$ over exactly one level spacing. For $D \ll 1$, we recover the Landauer formula for the resistance, $\widetilde{R}_q = \frac{h}{De^2}$ and the escape time is given by $\tau = h/D\Delta$, as expected from a semiclassical approach. The exponential current decay, the constant injection charge for $\tau \ll \mathcal{T}/2$, as well as the decrease of τ with transmission D , account well for our experimental observations in Fig.1B.

For a more accurate experimental determination of q and τ and to investigate subnanosecond time scales, we consider in the following measurements of the current first harmonic, I_ω , at higher frequencies $f = \omega/2\pi = 1/\mathcal{T}$. As a matter of fact, following Eq.1, we have:

$$I_\omega = \frac{2qf}{1 - i\omega\tau} \quad (4)$$

so that the modulus $|I_\omega|$ and the phase ϕ ($\tan(\phi) = \omega\tau$) allow for the determination of q and τ .

Fig.2A shows $|I_\omega|$ measured as a function of QPC gate voltage V_G at $f = 180$ MHz for increasing values of the excitation voltage $2eV_{exc}$. The range of V_G maps the full transmission excursion $D = 0-1$. The low excitation $2eV_{exc} = \Delta/4$ data nearly correspond to the linear response reported in Ref.[25]. The current exhibits strong oscillations reflecting the variation with V_G of the dot density of states at the Fermi energy. At larger excitation voltages, the current peaks are broadened as expected from Eq.2 when $2eV_{exc}$ gets larger than $k_B T$. For $2eV_{exc} = \Delta$, the oscillations disappear completely and $|I_\omega| = 2ef$, down to a low transmission threshold $D \sim 0.05$. The oscillations reappear for larger excitations. The constant current $|I_\omega| = 2ef$ is the frequency-domain counterpart of the constant charge regime observed in the time-domain, for the injection/absorption of a single electron per half period. The cut-off observed for $D \lesssim$

0.02 corresponds to the limit $\omega\tau \gtrsim 1$ where the escape time τ exceeds $\mathcal{T}/2$. The constant \widetilde{C}_q regime obtained for $2eV_{exc} = \Delta$ can be viewed on a striking manner in a Nyquist representation of Fig.2B. The corresponding diagram is the half-circle characteristic of an RC circuit with a constant capacitance e^2/Δ and transmission dependent resistance. By contrast the curves obtained for larger or smaller excitations exhibit strong capacitance oscillations.

Fig.2C represents the phase $\phi = \arctan(\omega\tau)$ of the current as a function of V_G for different excitation voltages. ϕ shows a quasi monotonic $\pi/2$ sweep in increasing transmission. The absence of significant oscillations proves that τ is nearly insensitive to the dot potential. As seen in the figure, τ is also independent of V_{exc} . In Fig.3, we have gathered the values of $\tau(V_G)$ obtained from 1GHz bandwidth time-domain measurements at 31.25 MHz repetition rate and from frequency-domain measurements at 180 and 515 MHz. The whole measurements probe a very broad transmission range ($D = 0.002 - 0.2$) corresponding to escape times varying from 10 ns to 100 ps. In the overlapping range, the different independent determinations coincide within error bars, agreeing quantitatively with the prediction $\tau = h/D\Delta$ also represented in Fig.3, where the dependence $D(V_G)$ is deduced from the linear regime [25].

We now discuss the conditions for single electron injection leading to a good quantization of the ac current as a figure of merit of single charge injection. Fig.4A represents $|I_\omega|$ as function of V_{exc} for typical values of the dc dot potential at fixed transmissions $D \approx 0.2$ and $D \approx 0.9$. Transmission $D \approx 0.2$ is low enough for the electronic states to be well resolved, as sketched in the inset of Fig.4A (left), but still large for the escape time to be shorter than $\mathcal{T}/2$. When the Fermi energy lies exactly in the middle of a density of states valley, we observe a well pronounced $|I_\omega| = 2ef$ current plateau centered on $2eV_{exc} = \Delta$. Whereas the current plateau resolution is noise limited to better than 1% (for a 10 seconds acquisition time), the plateau value is determined with an uncertainty of 5% due to systematic calibration error. We note that at this working point the plateau is robust upon variation of the parameters. By contrast, if the Fermi energy lies on a peak, there is still a current plateau but its value is arbitrary and very sensitive to parameter variations. These two working points illustrate the importance of having a well defined charge in the dot prior to injection. In the first case the charge is well defined and suit-

able for charge injection. In the second case the equilibrium dot charge fluctuates. In particular, when the energy level is exactly resonant with the Fermi energy, its mean occupation at equilibrium is $1/2$ and the measured value of the plateau is $1/2 \times 2ef = ef$ (see Fig.4A (left)). Thus, this working point is not suitable for a single electron source. Upon increasing transmission, even for a suitable working point, the dot charge quantization can be lost because of quantum fluctuations. First, the width of the ac current plateaus reduces and finally nearly vanishes for $D \approx 0.9$. Note that for different transmissions, all curves cross at $|I_\omega| = 2ef$ for $2eV_{exc} = \Delta$ reflecting the constant value of \widetilde{C}_q discussed above. Finally, domains of good charge quantization are best shown on the two-dimensional color plot of Fig.4.B-upper where the modulus of the current is represented in color scale. The vertical axis stands for the excitation voltage V_{exc} and the horizontal axis for the gate voltage V_G . The white diamonds correspond to large domains of constant current $|I_\omega| = 2ef$ suitable for single electron injection. At high transmissions the diamonds are blurred by dot charge fluctuations as discussed previously. On the opposite, for small transmissions, even when the dot charge quantization is good, current quantization is lost because of long escape time $\omega\tau \gg 1$, and the current goes to zero. At $180MHz$, optimal working conditions are obtained for $D \approx 0.2$. Experimental results of Fig.4 are compared with our theoretical model (Eqs.2 and 3) without any adjustable parameter (solid lines in Fig.4a and lower plot in Fig.4b)[30]. The agreement between measurements and theoretical predictions is excellent which shows that our single electron source lends itself to quantitative modeling.

The availability of a coherent source of single electrons emitted on demand from a single energy level on nanosecond time scale opens the way for a new generation of experiments never possible before. Synchronization of similar sources could be used in the future to probe electron anti-bunching, electron entanglement in multi-lead conductors or to generate electronic flying qubits in ballistic conductors.

The LPA is the CNRS-ENS UMR8551 associated with universities Paris 6 and Paris 7. The research has been supported by SESAME Ile-de-France and ANR-05-NANO-028 contracts.

-
- [1] A. Imamoglu, Y. Yamamoto, *Phys. Rev. Lett.* **72**, 210-213 (1994).
- [2] For a review see : N. Gisin, G. Ribordy, W. Tittel and H. Zbinden, *Rev. Mod. Phys.* **74**, 145-195 (2002).
- [3] P. Kok et al., *Rev. Mod. Phys.* **79**, 135-174 (2007).
- [4] A. Bertoni, P. Bordone, R. Brunetti, C. Jacoboni, and S. Reggiani, *Phys. Rev. Lett.* **84**, 5912-5915 (2000).
- [5] R. Ionicioiu, G. Amaratunga, and F. Udrea, *Int. J. Mod. Phys.* **15**, 125-133 (2001).
- [6] T. M. Stace, C. H. W. Barnes, and G. J. Milburn, *Phys. Rev. Lett.* **93**, 126804-7 (2004).
- [7] see for example: W. van Haeringen and D. Lenstra, *Analogies in Optics and Micro Electronics*, (Kluwer, Dordrecht, 1990).
- [8] M. Büttiker, *Phys. Rev B* **46**, 12485-12507 (1992).
- [9] Ya. M. Blanter and M. Büttiker, *Phys. Rep.* **336**, 2-166 (2000).
- [10] C. W. J. Beenakker, C. Emary, M. Kindermann, J. L. van Velsen, *Phys. Rev. Lett.* **91**, 147901-147904 (2003).
- [11] P. Samuelsson, E. V. Sukhorukov, and M. Büttiker, *Phys. Rev. Lett.* **92**, 026805-026808 (2004).
- [12] C.W.J. Beenakker, in *Quantum Computers, Algorithms and Chaos, International School of Physics Enrico Fermi*, (IOS Press, Amsterdam, 2006) vol. 162, edited by G. Casati, D.L. Shepelyansky, P. Zoller, and G. Benenti, pp. 307-347.
- [13] C. W. J. Beenakker and H. van Houten, *Solid State Physics* **44**, 1-228 (1991)
- [14] Y. Ji, Y. Chung, D. Sprinzak, M. Heiblum, D. Mahalu and H. Shtrikman, *Nature* **422**, 415-418 (2003)
- [15] single electrons detectors have been realized but are yet too slow compare with the electron transit time in the measurement leads.
- [16] B. J. van Wees et al., *Phys. Rev. Lett.* **60**, 848-850 (1988).
- [17] D. A. Wharam et al., *J. Phys. C* **21**, L209-214 (1988).
- [18] L. J. Geerligs et al., *Phys. Rev. Lett.* **64**, 2691-2694 (1990).

- [19] H. Pothier, P. Lafarge, C. Urbina and M.H. Devoret, *Europhys. Lett.* **17**, 249-254 (1992).
- [20] L. P. Kouwenhoven, A. T. Johnson, N. C. van der Vaart, and C. J. P. M. Harmans, *Phys. Rev. Lett.* **67**, 1626-1629 (1991).
- [21] A. Fujiwara, N.M. Zimmerman, Y. Ono, and Y. Takahashi, *Appl. Phys. Lett.* **84**, 1323-1325 (2004).
- [22] L. S. Levitov, H. Lee, and G. B. Lesovik, *J. Math. Phys.* **37** 4845 (1996)
- [23] T. Jonckheere, M. Creux, and T. Martin, *Phys. Rev. B* **72** 205321 (2005)
- [24] J. Keeling, I. Klich, and L. S. Levitov *Phys. Rev. Lett.* **97** 116403 (2006)
- [25] J. Gabelli, G. Fève, J.-M. Berroir, B. Placais, A. Cavanna, B. Etienne, Y. Jin, and D.C. Glattli, *Science* **313**, 499-502 (2006).
- [26] For additional experimental results see : G. Fève, Thesis, Université Pierre et Marie Curie (2006), (available at <http://tel.archives-ouvertes.fr/tel-00119589>).
- [27] M. Büttiker, H. Thomas, and A. Prêtre, *Phys. Lett.* **A180**, 364-369 (1993).
- [28] M. Büttiker, A. Prêtre, H. Thomas, *Phys. Rev. Lett.* **70**, 4114-4117 (1993).
- [29] A. Prêtre, H. Thomas, and M. Büttiker, *Phys. Rev. B* **54**, 8130-8143 (1996).
- [30] We use the 1D modeling of our circuit (density of states, transmission, dot-gates coupling) described in reference [25]

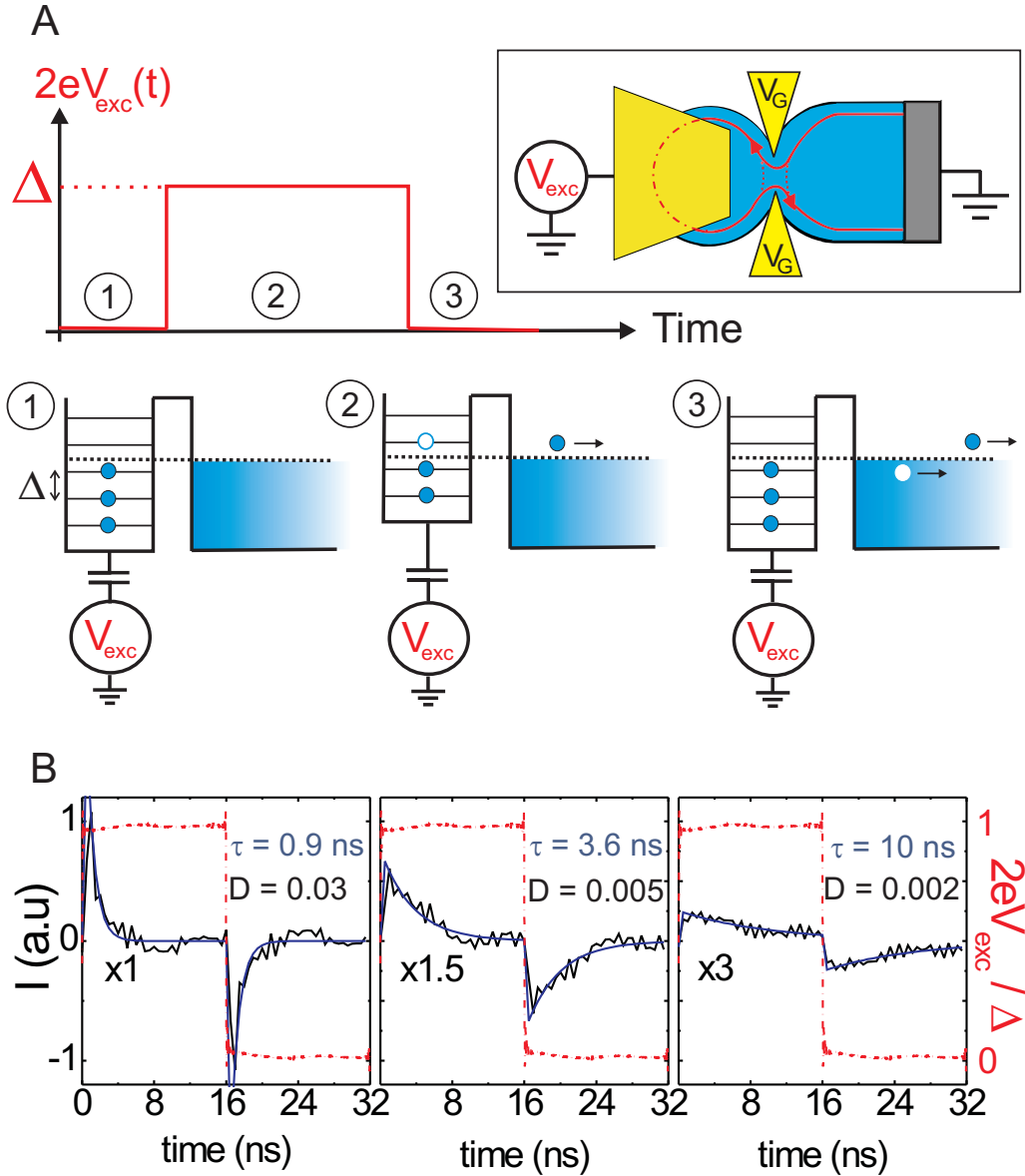


FIG. 1: Single charge injection. A) Schematic of single charge injection. Starting from an antiresonant situation where the Fermi energy lies between two energy levels of the dot (step 1), the dot potential is increased by Δ bringing one occupied level above the Fermi energy (step 2). One electron then escapes the dot on the mean time $\tau = \frac{\hbar}{D\Delta}$. The dot potential is then brought back to its initial value (step 3) where one electron can enter it, leaving a hole in the Fermi sea. Inset: The quantum RC circuit : one edge channel is transmitted inside the submicrometer dot with transmission D tuned by the QPC gate voltage V_G . The dot potential is varied by a radiofrequency excitation V_{exc} applied on a macroscopic gate located on top of the dot. The electrostatic potential can also be tuned by V_G due to the electrostatic coupling between the dot and the QPC. B) Time-domain measurement of the average current (black curves) on

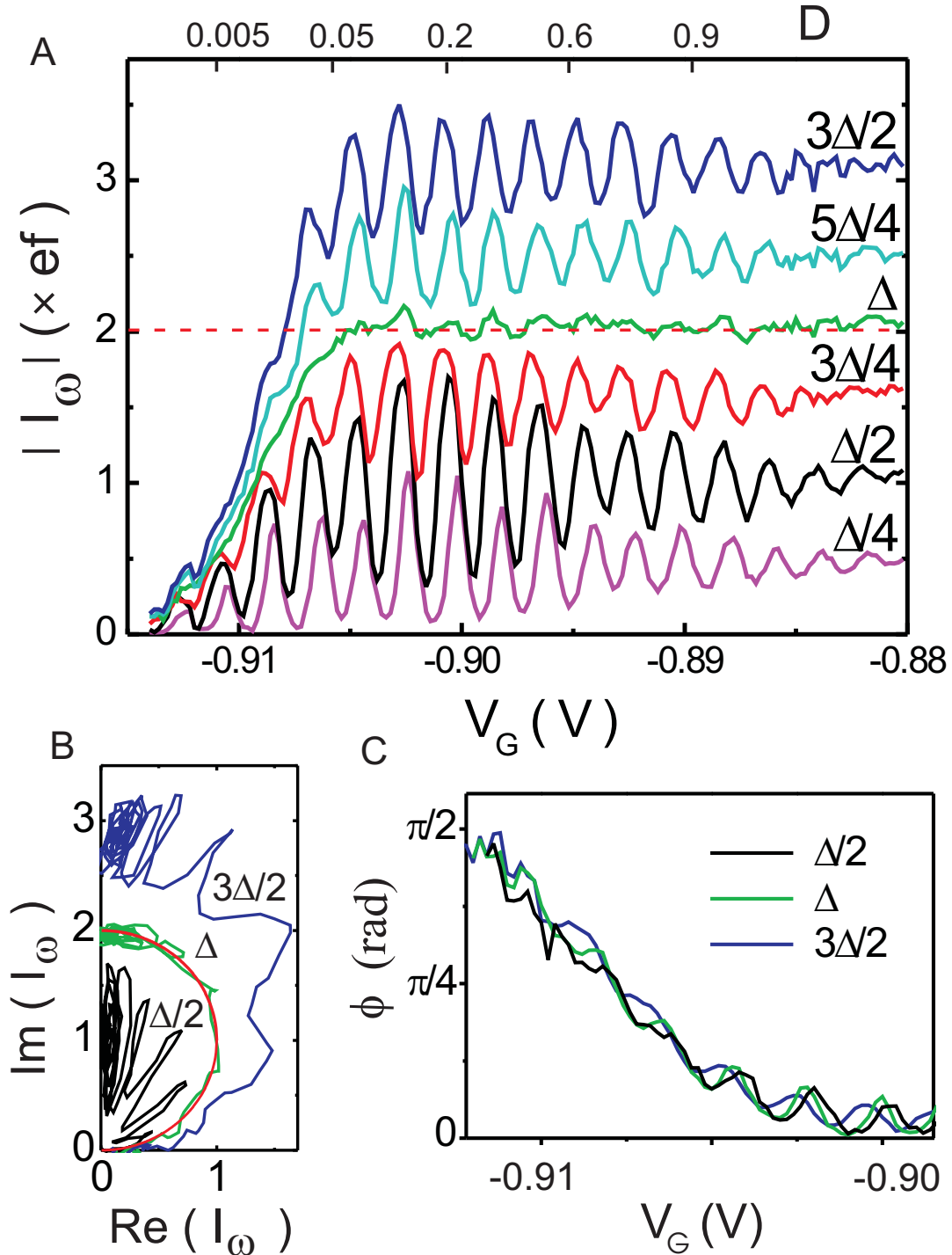


FIG. 2: I_ω as a function of V_G at $f = 180$ MHz for different values of the excitation amplitude $2eV_{exc}$. Transmission D is also indicated. A) Modulus $|I_\omega|$. The dashed line is the constant value $|I_\omega| = 2ef$. B) Nyquist representation ($\text{Im}(I_\omega)$ vs $\text{Re}(I_\omega)$). The red curve corresponds to an RC circuit of constant capacitance e^2/Δ and varying resistance. C) Phase ϕ . The phase ϕ is independent of V_{exc} .

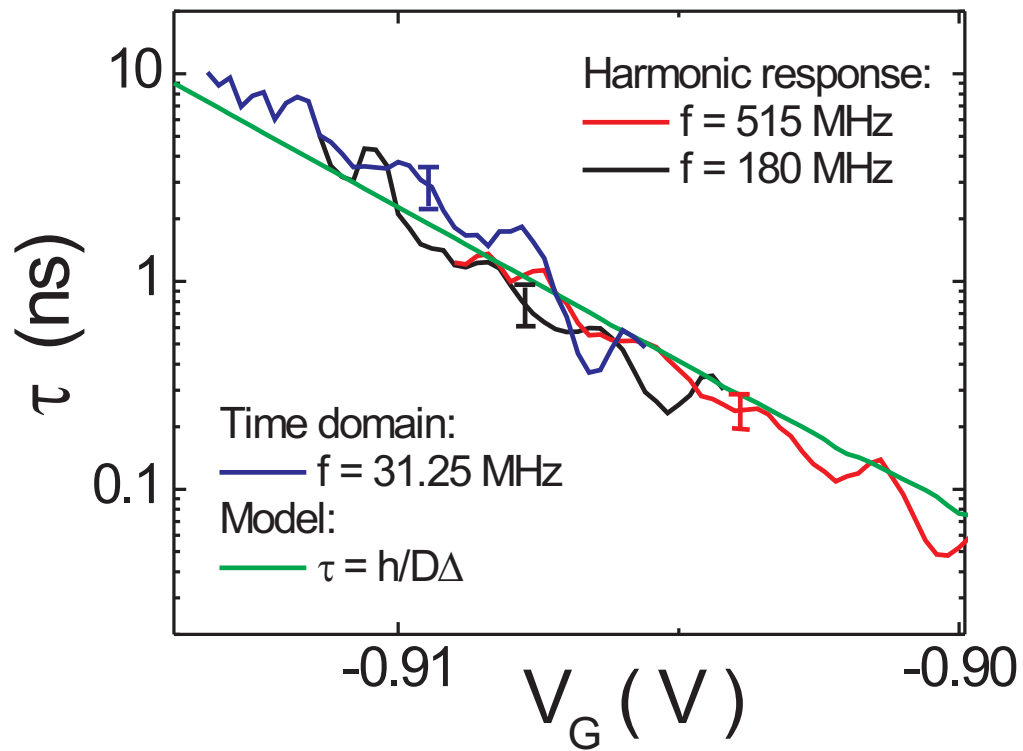


FIG. 3: Escape time τ in logarithmic scale as a function of QPC gate voltage V_G : experiments and model.

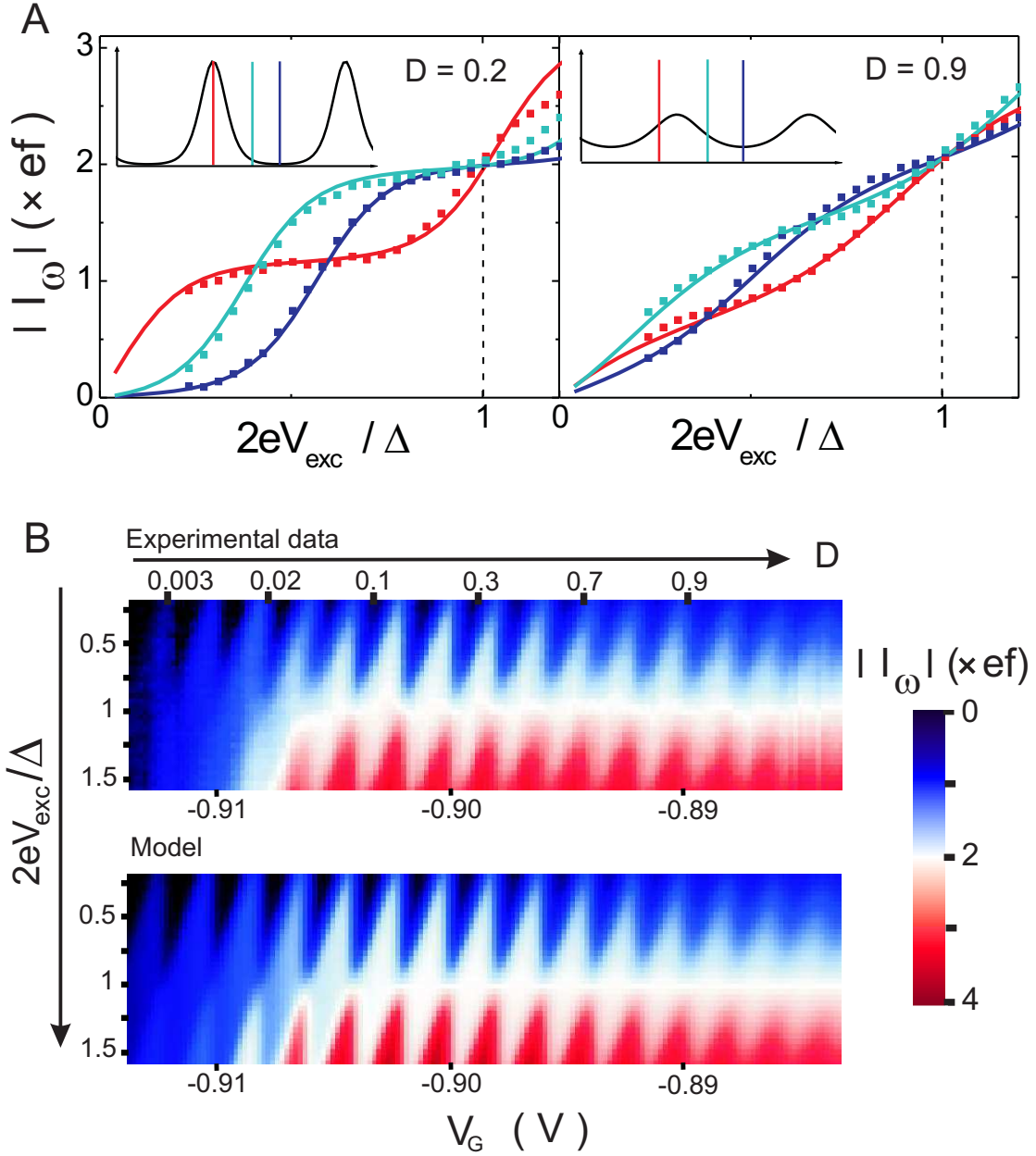


FIG. 4: Quantization of the ac current. A) $|I_\omega|$ as a function of $2eV_{exc}/\Delta$ for different dot potentials at $D \approx 0.2$ (left) and $D \approx 0.9$ (right). Points correspond to experimental values and lines to theoretical predictions. Insets: schematic representation of the dot density of states $N(\epsilon)$. The color bars indicate the dot potential for the corresponding experimental data. B) Color plot of $|I_\omega|$ as a function of $2eV_{exc}/\Delta$ and V_G : experiments (upper) and model (lower).